Title

ANALYSIS OF THE DISPLACEMENT VECTORS OF ANTIPHASE DOMAIN BOUNDARIES IN ANORTHITES (CaAl2Si2O8)

Authors

Muller, W.F.
Wenk, H.R.
Bell, W.L.
et al.

Publication Date

1972-12-01

Submitted to Mineralogy and Petrology

LBL-1457
Preprint

ANALYSIS OF THE DISPLACEMENT VECTORS OF ANTIPHASE DOMAIN BOUNDARIES IN ANORTHITES ($CaAl_2Si_2O_8$)

W. F. Müller, H. R. Wenk, W. L. Bell, and G. Thomas

December 1972

Prepared for the U. S. Atomic Energy Commission
under Contract W-7405-ENG-48

DISCLAIMER

ANALYSIS OF THE DISPLACEMENT VECTORS OF ANTIPHASE DOMAIN BOUNDARIES IN ANORTHITES ($CaAl_2Si_2O_8$)

W. F. Müller*

Department of Materials Science and Engineering

H. R. Wenk

Department of Geology and Geophysics and Space Sciences Laboratory

W. L. Bell** and G. Thomas

Inorganic Materials Research Division, Lawrence Berkeley Laboratory and Department of Materials Science and Engineering, College of Engineering; University of California, Berkeley, California

---

*Present address: Institut für Kristallographie, Universität, Frankfurt

**Present address: General Electric Company, Vallecitos Nuclear Center, Pleasanton, California

Abstract. As part of an electron microscopic study of plagioclase, displacement vectors for b- and c-domains have been determined from contrast experiments and calculations. In lunar anorthite from breccia 15459 (An 94.9), b-domains could only be imaged in dark field with b-reflections and c-domains only with c-reflections. The vector corresponding to these contrast conditions is ½[110] for b-domains and ½[111] for c-domains. The face centering vector ½[110] relates two domains with a reverse Al/Si arrangement. The body-centering vector ½[111] relates domains of identical Al/Si distribution but different atomic coordinates. Fringe patterns for c-domains have been obtained for Pasmeda anorthite. Calculated intensity profiles applying multi-beam dynamic theory and a ½[111] displacement vector are in agreement with the observations.

INTRODUCTION

Recent transmission electron microscopic studies of the feldspars bytownite and anorthite have revealed antiphase domains up to some microns in diameter which were separated by antiphase domain boundaries (Christie *et al.*, 1971; Czank *et al.*, 1972; Heuer *et al.*, 1972; Lally *et al.*, 1972; Müller *et al.*, 1972; Müller and Wenk, 1973 ; Wenk *et al.*, 1972). While such domains were directly seen for the first time in the transmission electron microscope, X-ray crystallographers had postulated their presence years prior to such observations (Goldsmith and Laves, 1955; Megaw, 1962; for a review of structural studies on feldspars the reader is referred to the paper by Smith and Ribbe, 1969).

Two different types of antiphase domain boundaries (APBs) occur: type b-APBs, which may be imaged with type b-reflections ($h + k$ odd, ℓ odd) and type c-APBs which may be imaged with type c-reflections ($h + k$ even, ℓ odd). Clearly resolvable c-APBs have been observed in anorthites with a chemical

composition between An 92 ($Na_{0.08}Ca_{0.92}Al_{1.92}Si_{2.08}O_8$) and An 100 ($CaAl_2Si_2O_8$). Type b-APBs have been found in bytownites and anorthites in a composition range of about An 80 to An 95.

In this paper, we report on the analysis of the displacement vectors of both types of antiphase domain boundaries in anorthites by transmission electron microscopy. The antiphase or displacement vector of an APB separating two domains is the vector which translates the lattice of one domain into that of the other. APBs in a crystal may be formed by deformation or may be caused by ordering processes which take place during cooling (for literature, cf. Marcinkowski, 1963). We deal in this paper with the latter case. The terms antiphase domain and APB are used here not as strictly as metallurgists might do (compare Christie *et al.*, 1971). That is, we do not exclude that the APBs are due to phase changes from a crystal with higher to lower symmetry which involve not only ordering of statistically distributed atoms to distinct lattice sites but may also cause some changes of atomic coordinates. Therefore, the displacement vector may be an imperfect lattice vector.

EXPERIMENTAL

A Hitachi HU 650 electron microscope with 650 kV acceleration voltage was used for this study. It was equipped with an orthogonal high-angle tilting stage which permitted tilting up to ±25° (Bouchard *et al.*, 1973). Suitably thin electron transparent foils were prepared from conventional petrographic thin sections by ion-bombardment (Barber, 1970). Specific conditions are described by Müller and Wenk (1973).

CRYSTAL STRUCTURE

Anorthite, $CaAl_2Si_2O_8$, crytallizes in the space group $P\bar{1}$. Its unit

cell is primitive and the c-axis (14 Å) about twice that of the feldspars albite or microcline which are described in a C-face-centered structure (Taylor, 1933; Taylor *et al.*, 1934). Structure analyses of anorthite were done by Kempster *et al.* (1962) and Megaw *et al.* (1962); a structure refinement was conducted by Wainwright and Starkey (1971). The unit cell of anorthite consists of four subcells of equal volume with the c-axis of 7 Å. It was found that Si and Al tetrahedra alternate so that each oxygen atom has one Si and one Al as neighbors, i.e., Si and Al are perfectly ordered. Pairs of subcells related by the body-centering vector $\frac{1}{2}[\underline{a} + \underline{b} + \underline{c}]$ have the same Si-Al distribution, but differ in their atomic coorinates. On the othe hand, pairs of subcells related by the C-face-centering vector $\frac{1}{2}[\underline{a} + \underline{b}]$ have similar atomic coordinates but an exactly reversed Si-Al arrangement.

The X-ray reflections of anorthite have been classified as type a ($\underline{h} + \underline{k}$ even, $\underline{\ell}$ even), b ($\underline{h} + \underline{k}$ odd, $\underline{\ell}$ odd), c ($\underline{h} + \underline{k}$ even, $\underline{\ell}$ odd), and d ($\underline{h} + \underline{k}$ odd, $\underline{\ell}$ even) (Gay, 1953). Type a-reflections are the only reflections present in alkalifeldspars; b-reflections have been attributed to Si-Al order (Laves and Goldsmith, 1955) and are also present in bytownites (An 80 to 90), and they become increasingly weak with decreasing An-contents and split up (e-reflections in intermediate plagioclase). The crystal structure with only a- and b-reflections has been called body-centered anorthite. Anorthite with sharp c- (and the much weaker d-) reflections is called primitive anorthite and that with diffuse c-reflections transitional anorthite. The boundaries between these types of structure are gradational.

DIFFRACTION CONTRAST ANALYSIS OF ANTIPHASE-DOMAIN BOUNDARIES

Lattice displacements modify the scattering potentials of the crystal

and introduce phase dependences of $\alpha = 2\pi\bar{g} \cdot \bar{R}(z)$ into the diffracted electron amplitudes ($\bar{g}$ = reciprocal lattice vector for the reflection operating, $\bar{R}(z)$ = displacement). For simple planar defects such as stacking faults and antiphase boundaries (APBs), the displacement vector $\bar{R}(z)$ changes abruptly only across the discontinuity plane and remains constant otherwise. This change in displacement is a crystal parameter and is the same for all diffracted beams. However, the change in phase angle, $\Delta\alpha$, varies due to the different reciprocal lattice vectors associated with different diffracted beams. For example, the transmitted beam with rel-vector $\bar{g} = (000)$ never has phase changes introduced by displacements of defects of any sort since $\Delta\alpha = \alpha \equiv 0$ in all cases. Often with planar defects the situation arises wherein diffracted beams will have phase changes $\Delta\alpha = n2\pi$, $n = \bar{g} \cdot \bar{R}$ an integer, and there will be no direct influence of the planar defect upon these diffracted beams.

Contrast from these defects arises through dynamic interactions with beams for which $\alpha \neq n2\pi$. The bright-field image of an inclined plane will only exhibit fringes if there is at least one diffracted beam whose phase was influenced by the discontinuity plane. From the viewpoint of the simple two-beam dynamic theory, APBs would be invisible if a fundamental reflection (a) were excited and would exhibit fringes in both bright-field and dark-field if a superlattice reflection (b or c) were excited.

Because of the size of the unit cell in anorthite, it is unlikely that two-beam conditions would ever be realizable at any voltages commonly encountered in transmission electron microscopy. The contrast experiments for this report were performed at 650 kV where multiple-beam interactions, both systematic and simultaneous, were unavoidable.

In order to estimate the contrast to be expected for the various APBs in multiple-beam situations, a computer program capable of calculating the results of such interactions was specially modified to handle the treatment of a triclinic unit cell with a large number of atoms and a variety of species (for formulae see Van Landuyt *et al.*, 1964; and the review of Amelinckx, 1970). Atomic species, positions, lattice parameters, and temperature factors were obtained from Wainwright and Starkey (1971). Electron scattering factors were obtained from standard tables (Hirsch *et al.*, 1971). The ratio of the mean and anomalous absorption parameters was estimated as 0.67.

THE DISPLACEMENT VECTOR OF b-APBs

Type b-APBs occurring in calcic plagioclases from lunar basalts were first observed by Christie *et al.* (1971). These authors report that APBs were in contrast using b-reflections and out of contrast with a- and c-reflections. They attribute the b-APBs to subsolidus ordering of Si-Al and conclude that the antiphase vector is $\frac{1}{2}[001]$. If this were the case, the b-APBs should be observable also in the light of type c-reflections, because both b- and c-reflections would give $\alpha = \pm \pi \bmod 2\pi$ for $R = \frac{1}{2}[001]$. In a later paper, Heuer *et al.* (1972) attribute the failure to image b-APBs with c-reflections to their weakness and diffuseness. In fact, the b-APBs observed so far (Christie *et al.*, Heuer *et al.*, 1972; Lally *et al.*, 1972; Müller *et al.*, 1972; Wenk *et al.*, 1972) occurred in bytownites and anorthites (An <95) which had diffuse and relatively weak c-reflections. Hence, it was not possible until now to conduct conclusive diffraction contrast experiments in order to solve the problem.

We found now in an anorthite crystal (An 92.5) from lunar breccia 15459, 0.05 mm in diameter, both type b- and type c-APBs, the c-reflections being

relatively intense and sharp (Figure 1). This has permitted the determination of the displacement vectors of both types of APBs.

Contrast experiments showed that the b-APBs were out of contrast using a- and c-reflections. For illustration, the phase factors α calculated for several operating reflections g- and for the displacement vectors $\frac{1}{2}[001]$, $\frac{1}{2}[110]$, and $\frac{1}{2}[111]$ are given in Table 1. According to visibility- and invisibility-criteria the displacement vector is $\frac{1}{2}[110]$ for the b-APBs and $\frac{1}{2}[111]$ for c-APBs.

Figure 1a displays the smoothly curved b-APBs which are generally larger than the more rugged c-APBs in this crystal (Figure 1b). Dark field micrographs simultaneoulsy imaged with a b- and c-reflection show that in the Bragg contour of the b-reflection only the b-APBs are in contrast and in the Bragg contour of the c-reflection only the c-APBs (Figure 2).

THE DISPLACEMENT VECTOR OF c-APBs AND EXAMINATIONS OF FRINGE CONTRAST

The electron microscope study of APBs in the anorthite from Val Schiesone, Alps (An 97) led Müller *et al.* (1972) to the conclusion that the antiphase vector of c-APBs is $\frac{1}{2}[111]$, since the APBs were in contrast with c-reflections operating and out of contrast with a- and b-reflections. The displacement vector $\frac{1}{2}[111]$ was predicted by Ribbe and Colville (1968). Our studies of anorthite from Val Pasmeda, S. Tyrol (An 100) and of an anorthite from lunar breccia 15459 (An 92.5) confirmed the previous results. Fringe patterns provided additional evidence. Figure 3 shows c-APBs in the anorthite from Val Pasmeda; Figure 4 shows a selected area from Figure 3 in bright field and in dark field using

a- and c-reflections to image the domains. Intensity profiles have been calculated applying multi-beam dynamic theory.

One of the characteristics of an APB, as opposed to a stacking fault, is that anomalous absorption effects are not readily observable in images of the defect. That is, the dark-field image of an APB may not be apparently asymmetric even though extremely thick foils are used. Computed intensity profiles (Figure 5) are in agreement with observations (Figure 4), and only a slight amount of dark-field asymmetry may be detected.

An APB would not normally be expected to be detectable with an a-reflection such as for $g = 22\bar{2}$, even though the boundary is in strong contrast for the first order image ($g = 11\bar{1}$). This is so because the phase angle for the second order reflection is 2π radians (i.e., $g \cdot R = 1$). However, under strong multiple-beam conditions wherein systematic or simultaneous reflections are unavoidable, the unexpected image would appear by double diffraction (i.e., dynamic interaction with other diffracted beams). Hence, Figure 5 also shows the fairly strong dark-field profile for an APB in the $22\bar{2}$ image. This profile is asymmetric since strong anomalous absorption effects are associated with this reflection.

Although the computer profiles are shown for a foil thickness of only two extinction distances, which may seem a small number, it must be remembered that extinction distances for reflections capable of detecting APBs are generally quite large. For the $11\bar{1}$ reflection at 650 kV the extinction distance is 5950 Å (computer calculated for relativistic electron scattering from anorthite) and the foil thickness for an image with a similar number of APB fringes would be 1.2 microns, a very thick foil indeed.

Equipped with the above information, it is possible to determine the

displacement vector of antiphase boundaries. Strong visibility of APB fringes can be obtained, in bright-field and dark-field images, by orienting the diffracting crystal so that a reflection is strongly excited for which the phase angle change produced by the boundary is an odd multiple of π radians; otherwise, near or complete invisibility of the boundary will occur. Very thick foils must be used to obtain even a few image fringes because of the extremely large extinction distances associated with reflection suitable for imaging APBs. Images are easily distinguished from those of other planar defects both by the invisibility criteria and the image character werein anomalous absorption effects are not strongly evident, and both bright- and dark-field images are symmetrical about the foil center. The APB fringe images are complimentary in the two fields; the central fringe being bright in bright-field and dark in dark-field images.

DISCUSSION AND CONCLUSIONS

Two different types of antiphase domain boundaries (APBs) in anorthites have been observed by transmission electron microscopy: the displacement vector of b-APBs was determined as $\frac{1}{2}[110]$. This vector is in agreement with structural considerations since it relates sublattices of similar atomic coordinates but exactly reversed Si-Al arrangements, i.e., the formation of b-APBs is connected with Si-Al ordering (Laves and Goldsmith, 1955; see also Christie *et al.*, 1971). It is likely that $\frac{1}{2}[110]$ (and not $\frac{1}{2}[001]$ as suggested by Christie *et al.*, 1971, and Heuer *et al.*, 1972) is the displacement vector for b-APBs not only in the anorthite An 92.5 from lunar breccia 15549 but also in calcic plagioclases which have diffuse c-reflections. In the truly body-centered structure, of course, the antiphase domain vectors $\frac{1}{2}[110]$ and $\frac{1}{2}[001]$ would describe identical situations.

The antiphase vector of c-APBs was found to be 1/2 [111]. Structural considerations suggested also this antiphase vector (cf. Goldsmith and Laves, 1955; Megaw, 1962; Ribbe and Colville, 1968). Heuer, et al. (1972) mention that the c-APBs are also in contrast with type d-reflections. This is to be expected for the displacement vector 1/2 [111].

On the basis of these structural facts in calcic plagioclase we can speculate about some processes during cooling of an igneous rock. At a very high temperature the Al/Si distribution is partially disordered. Upon cooling ordered domains with reversed Al/Si arrangement are produced and these domains are separated by b-APBs. The displacement vector has been determined as 1/2 [110] which is equivalent to 1/2 [001] in a truly body-centered structure. It may be that b-domains are only found in plagioclase with an initially disordered Al-Si distribution such as in lunar basalt. Upon further cooling positional order of Ca causes c-APBs with a displacement vector 1/2 [111]. In the light of recent investigations (Muller and Wenk, 1973) the conditions under which c-domains form are still uncertain, and it is not unlikely that both b- and c-domains are produced during Al/Si ordering at high temperatures.

---

[1] Dr. H. Schulz informed us that a structural interpretation of c-domains will be published by Czank, Van Landuyt, Schulz, Laves and Amelinckx in Z. Kristallogr. (title of the paper: Electron Microscopy Study of the Structural Changes as a Function of Temperature in Anorthite).

ACKNOWLEDGEMENTS

We wish to thank Dr. J. E. Wainwright (Houston) for the Pasmeda anorthite sample. The work was supported by NASA grant NGL 05-003-410 to H.-R. Wenk, W. F. Müller thanks the Deutsche Forschungsgemeinschaft for a research stipend. We acknowledge the continued support of the U. S. Atomic Energy Commission through the Lawrence Berkeley Laboratory. We also thank Dr. M. Bouchard, D. Jurrica, W. Wilde, T. Astrup. G. Stone, and O. Van der Biest for valuable discussions and help with the electron microscope. The computer center at Berkeley provided some subsidized computer time.

REFERENCES

Amelinckx, S.: The study of planar interfaces by means of electron microscopy. In: Modern diffraction and imaging techniques in materials science (S. Amelinckx, R. Gevers, G. Remaut, J. Van Landuyt, eds.), pp. 257-294. Amsterdam-London: North Holland Publ. Co. (1970).

Barber, D. J.: Thin foil of non-metals made for electron microscopy by sputter-etching. J. Mat. Sci., 5, 1-8 (1970).

Bouchard, M., Worthington, W. L., Jurica, D. J., Swann, P. R.: A high angle tilting stage for the 650 kV Hitachi microscope. Review Sci. Instr. (1973, in press).

Christie, J. M., Lally, J. S., Heuer, A. H., Fisher, R. M., Griggs, D. T., Radcliffe, S. V.: Comparative electron petrography of Apollo 11, Apollo 12 and terrestrial rocks. Proc. Second Lunar Sci. Conf. Geochim. Cosmochim. Acta, Suppl. 2, vol. 1, 69-89. MIT Press (1971).

Czank, M., Schulz, H., Laves, F., and Gross, W.: Investigation of domains in anorthite by electron microscopy. Naturwiss., 59, 77-78 (1972).

Gay, P.: The structures of plagioclase feldspars: III. An X-ray study of anorthites and bytownites. Mineral Mag., 30, 169-177 (1953).

Goldsmith, J. R., Laves, F.: Cation order in anorthite ($CaAl_2Si_2O_8$) as revealed by Gallium and Germanium substitutions. Z. Krist., 106, 213-226 (1955).

Heuer, A. H., Lally, J. S., Christie, J. M., Radcliffe, S. V.: On phase transformations and exsolution in lunar and terrestrial plagioclases. Phil. Mag., 26, 465-482 (1972).

Hirsch, P. B., Howie, A., Nicholson, R. B., Pashley, D. W., Whelan, M. J.: Electron microscopy of thin crystals. Butterworths, London (1971).

Kemster, C. J. E., Megaw, H. D., Radoslovich, E. W.: The structure of anorthite, $CaAl_2Si_2O_8$. I Structure Analysis. Acta Cryst., 15, 1005-1017 (1962).

Lally, S., Fisher, R. M., Christie. J. M., Griggs, D. T., Heuer, A. H., Nord, G. L., Jr., Radcliffe, S. V.: Electron petrography of Apollo 14 and 15 rocks. Proc. Third Lunar Science Conf. Geochim. Cosmochim. Acta, Suppl. 3, vol. 1, 401-422, MIT Press (1972).

Laves, F., Goldsmith, J. R.: The effect of temperature and composition on the Al-Si distribution in anorthite. Z. Krist., 106, 227-235 (1955).

Marcinkowski, J. M.: Theory and direct observation of antiphase boundaries and dislocations in superlattices. In: Electron microscopy and strength of materials (G. Thomas and J. Washburn, eds.). 330-440. Interscience Publishers (1963).

Megaw, H. D.: Order and disorder in feldspars. Norsk. Geol. Tidsskr., 42/2, 104-137 (1962).

Megaw, H. D., Kempster, C. J. E., and Radoslovich, E. W.: The structure of anorthite $CaAl_2Si_2O_8$. II Description and discussion. Acta Cryst., 15, 1017-1035 (1962).

Müller, W. F., Wenk, H. R., Thomas G.: Structural variations in anorthites. Contr. Mineral. Petrol., 34, 304-314 (1972).

Müller, W. F., and Wenk, H. R.: Changes in the domain structure of anorthites induced by heating. N. Jb. Mineral. Petrog. (in press, 1973).

Ribbe, P. H., Colville, A. A.: Orientation of the boundaries of out-of-step domains in anorthite. Mineral. Mag., 36, 814-819 (1968).

Smith, J. V., Ribbe, P. H.: Atomic movements in plagioclase feldspars. Contr. Mineral. and Petrol., 21, 157-202 (1969).

Taylor, W. H. The structure of sanidine and other feldspars. Z. Krist., 85, 425-442 (1933).

Taylor, W. H., Darbyshire, J. A., Strunz, H.: An X-ray investigation of the feldspars. Z. Krist., 87, 464-498 (1934).

Van Landuyt, J., Gevers, R., Amelinckx, R.: Fringe patterns at antiphase boundaries with $\alpha = \pi$ observed in the electron microscope. Phys. Stat. Sol., 7, 519-546 (1964).

Wainwright, J. E., Starkey, J.: A refinement of the structure of anorthite. Z. Krist., 133, 75-80 (1971).

Wenk, H. R., Ulbrich, M., and Müller, W. F.: Lunar plagioclase (a mineralogical study). Proc. Third Lunar Sci. Conf. Geochim. Cosmochim. Acta, Suppl. 3, vol. 1, 569-579, MIT Press (1972).

TABLE 1. PRINCIPAL VALUES OF THE PHASE FACTOR $\alpha = 2\pi g \cdot \underline{R}$ (g = REFLECTION OPERATING, $\underline{R}$ = DISPLACEMENT VECTOR FOR SOME REFLECTIONS, AND OBSERVED CONTRAST OF ANTIPHASE DOMAIN BOUNDARIES IN ANORTHITE FROM LUNAR BRECCIA 15459.

	α			Observed Contrast	
g	R = ½[001]	R = ½[110]	R = ½[111]	*b*-APBs in Contrast?	c-APBs in Contrast?
020	0	2π	2π	no	no
$20\bar{2}$	2π	2π	0	no	no
$10\bar{1}$	π	π	0	yes	no
$12\bar{5}$	π	π	2π	yes	no
$21\bar{3}$	π	π	2π	yes	no
$20\bar{3}$	π	2π	π	no	yes
$31\bar{5}$	π	2π	π	no	yes
$31\bar{3}$	π	2π	π	no	yes

FIGURE CAPTIONS

Figure 1. Transmission electron micrograph of APBs in an anorthite crystal (An 92.5) from lunar breccia 15459. (a) Type b-APBs. (b) Type c-APBs. Dark-field images, 650 kV. Diffraction patterns are inserted and $\bar{g}$ vectors are indicated.

Figure 2. Dark-field image of b- (right) and c- (left) APBs (same crystal as in Figure 1). The reflections $\underline{g} = 20\bar{3}$ and $21\bar{3}$ are operating simultaneously (see text). 650 kV.

Figure 3. Type c-APBs in an anorthite (An 100) from Val Pasmeda, S. Tyrol. Dark-field image with $\underline{g} = 13\bar{1}$ operating. 650 kV.

Figure 4. Type c-APBs in bright field (a) and dark field with $11\bar{1}$ (b) and $22\bar{2}$ (c) as operating reflections (selected area from Figure 3). Note contrast characteristics for $\alpha = \pi$ fringes. 650 kV. Diffraction pattern inserted.

Figure 5. Computed multi-beam intensity profile across a c-APB using dynamic theory. Profiles for bright field and dark field with $11\bar{1}$ (c) and $22\bar{2}$ (a) as operating reflections. $\frac{1}{2}[111]$ is the assumed displacement vector. Conditions correspond to the case shown in Figure 4 (direction of foil normal = [314], accelerating voltage = 650 kV, corrected extinction distance = 1.61 Å, electron wavelength = 0.0119 Å, ratio mean/anomalous absorption parameters = 0.67, sixbeam case: 000, $11\bar{1}$; $22\bar{2}$; $1\bar{1}1$; 5 13 $\bar{7}$; $\bar{1}\bar{3}$ 3 9).

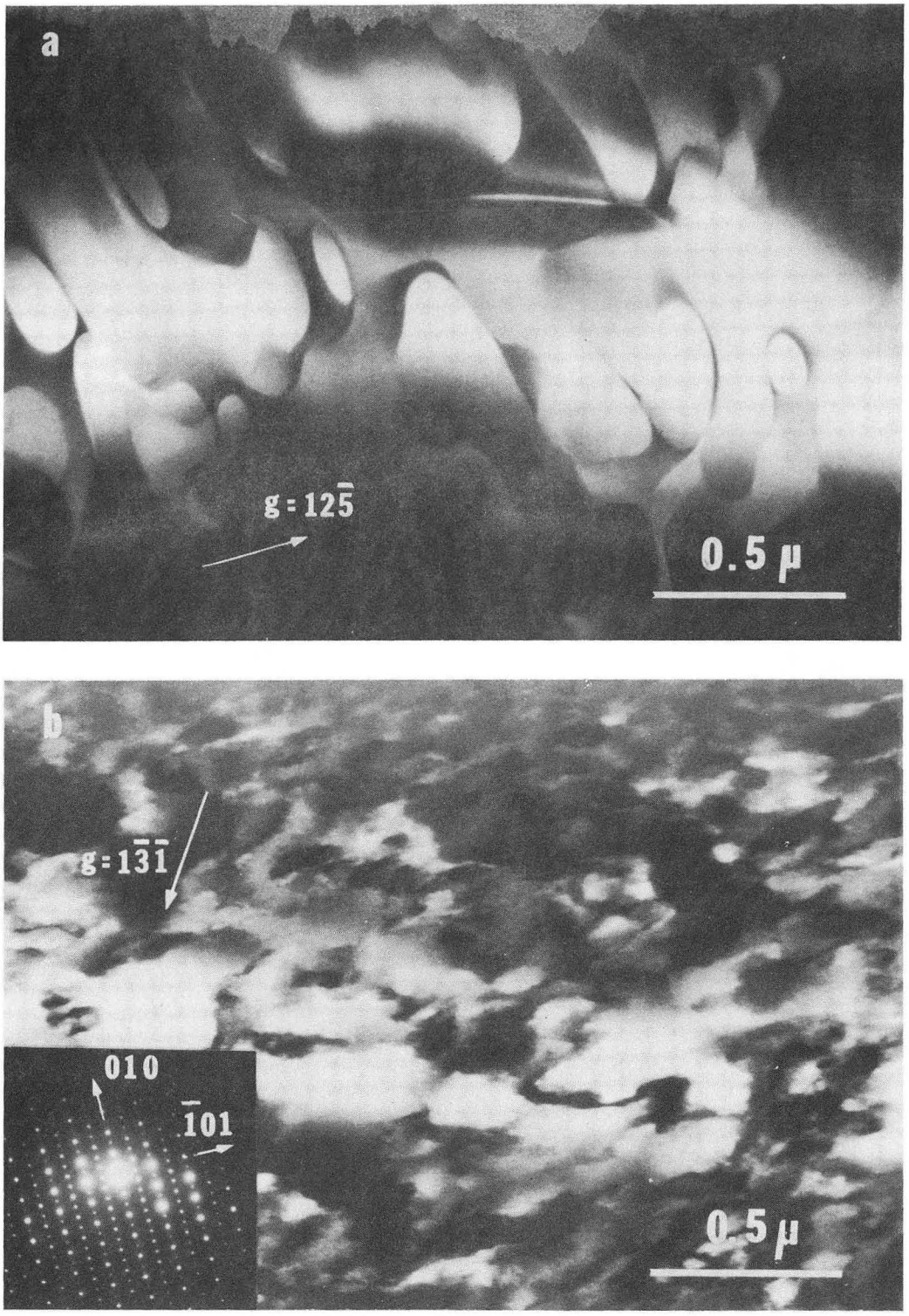

XBB 728-4150

Fig. 1

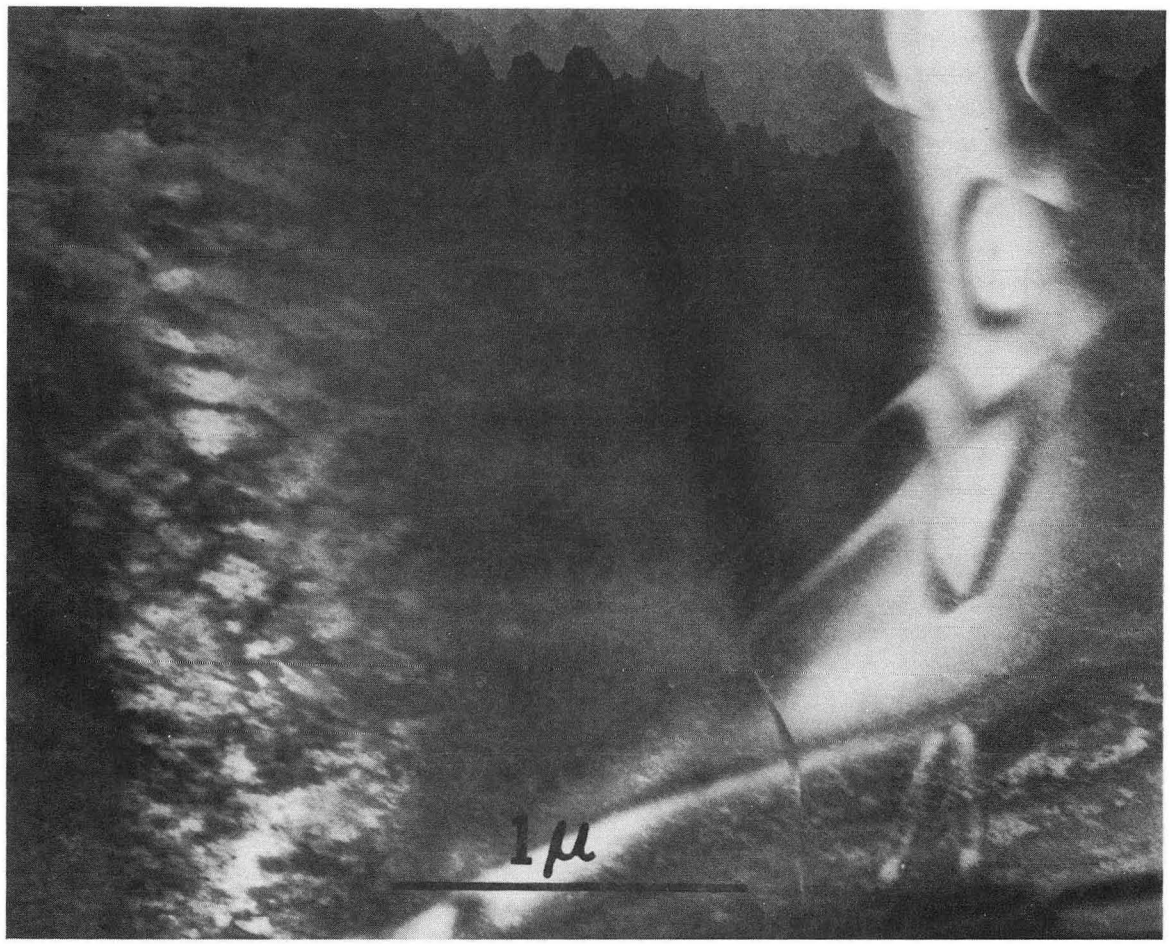

XBB 732-865

Fig. 2

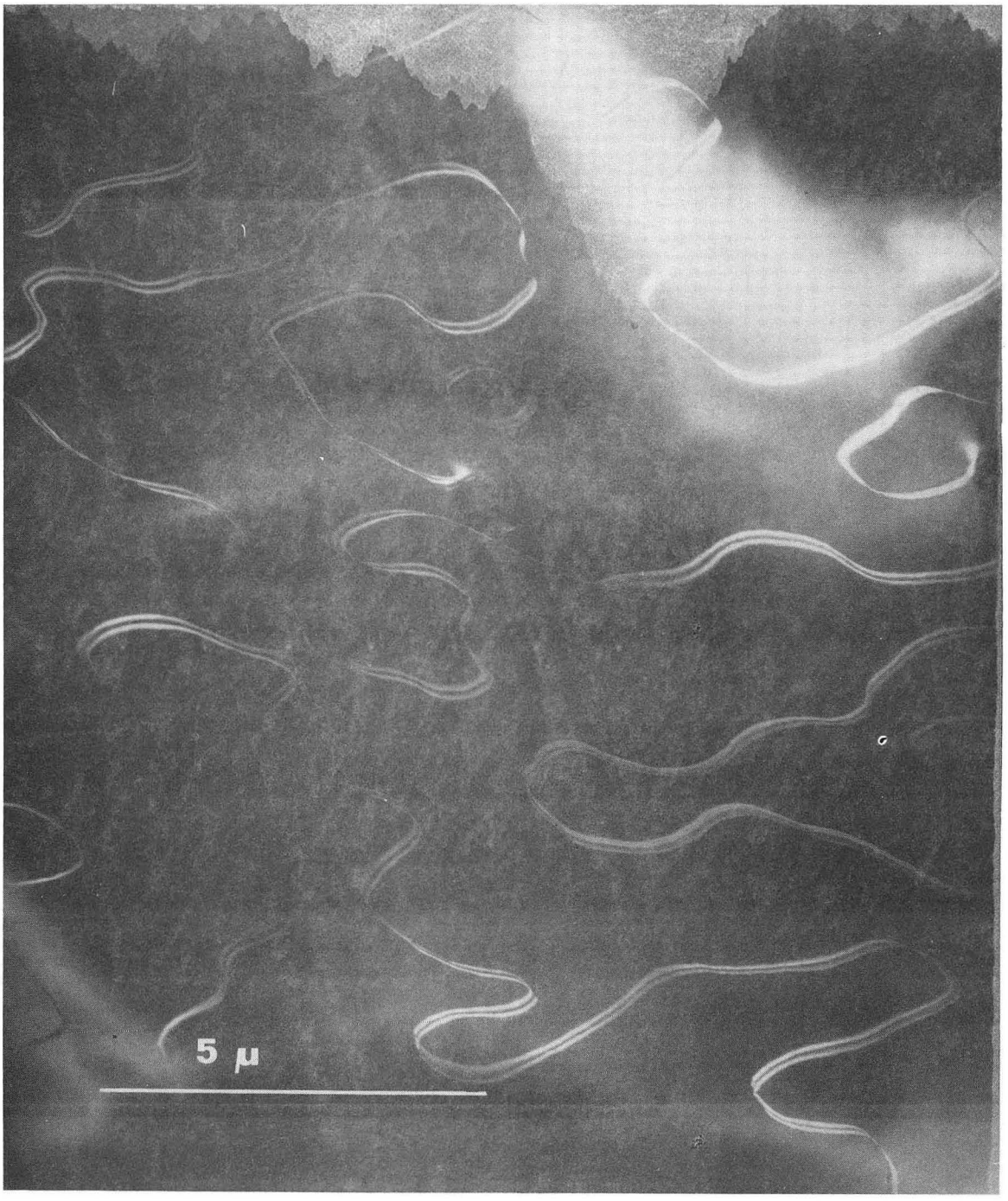

XBB 728-4152

Fig. 3

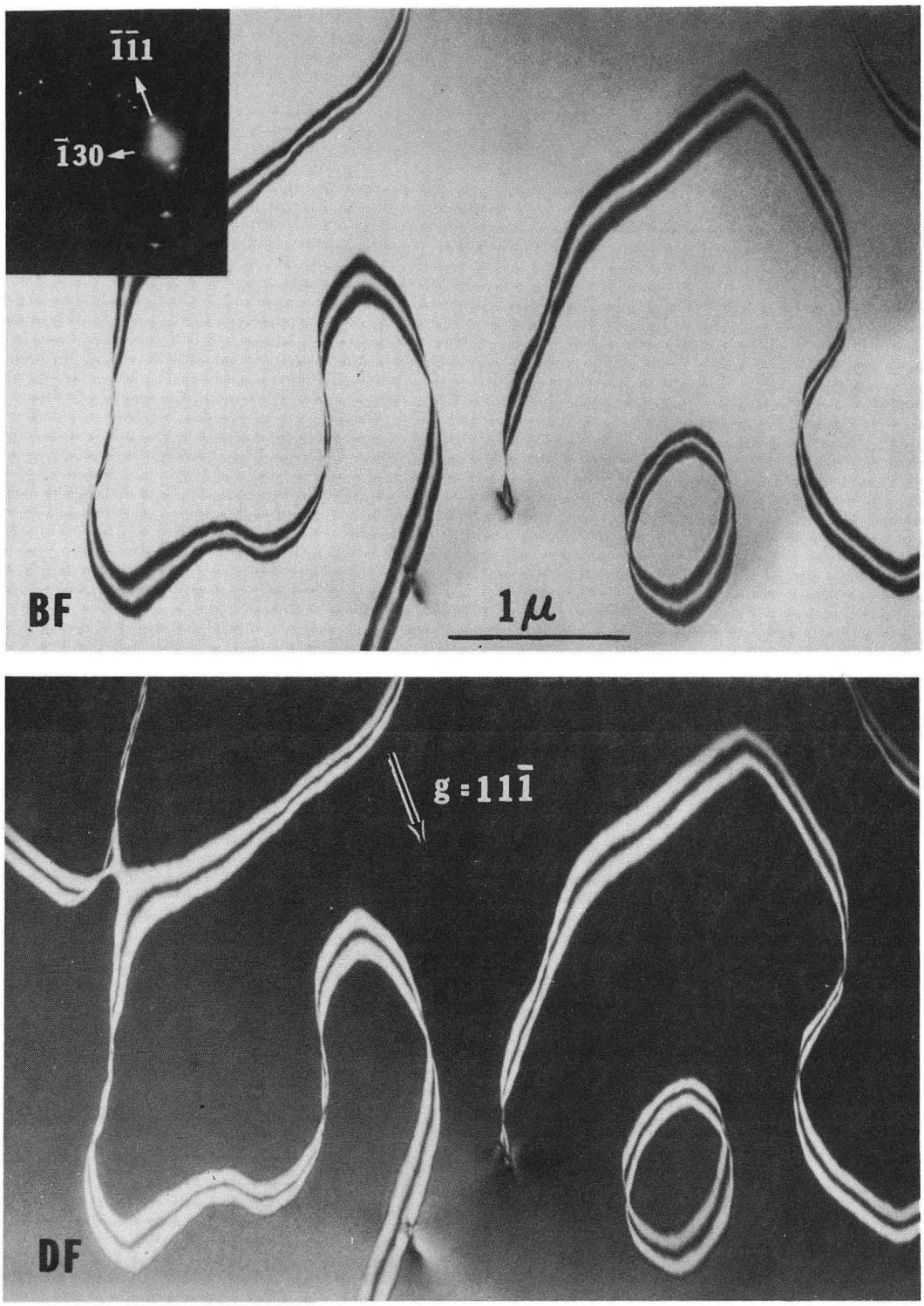

XBB 728-4149

Fig. 4

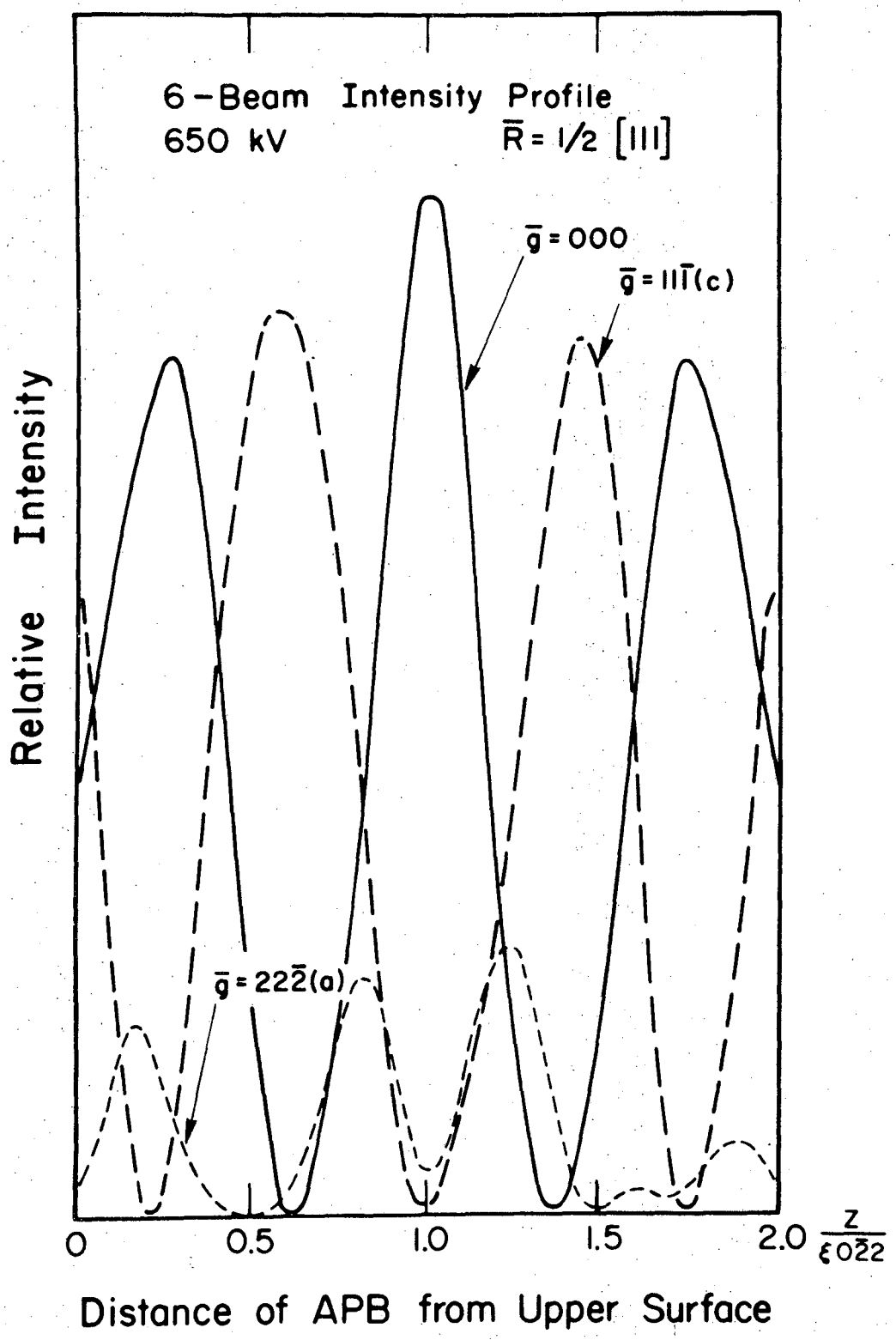

XBL 732-5764

Fig. 5

TECHNICAL INFORMATION DIVISION
LAWRENCE BERKELEY LABORATORY
UNIVERSITY OF CALIFORNIA
BERKELEY, CALIFORNIA 94720